Manuscript prepared for Atmos. Chem. Phys.
with version 5.0 of the LaTeX class copernicus.cls.
Date: 13 October 2015

Reactive nitrogen partitioning and its relationship to winter ozone events in Utah

R. J. Wild[1,2], P. M. Edwards[1,2,*], T. S. Bates[3,4], R. C. Cohen[5], J. A. de Gouw[1,2], W. P. Dubé[1,2], J. B. Gilman[1,2], J. Holloway[1], J. Kercher[6], A. R. Koss[1,2], L. Lee[4], B. M. Lerner[1,2], R. McLaren[7], P. K. Quinn[3], J. M. Roberts[2], J. Stutz[8], J. A. Thornton[9], P. R. Veres[1,2], C. Warneke[1,2], E. Williams[2], C. J. Young[1,2,**], B. Yuan[1,2], K. J. Zarzana[1,2], and S. S. Brown[2,10]

[1]Cooperative Institute for Research in the Environmental Sciences, University of Colorado, Boulder, Colorado 80309, USA
[2]Chemical Sciences Division, Earth System Research Laboratory, National Oceanic and Atmospheric Administration, Boulder, Colorado 80305, USA
[3]Pacific Marine Environmental Laboratory, National Oceanic and Atmospheric Administration, Seattle, Washington 98115, USA
[4]Joint Institute for the Study of the Atmosphere and Oceans, University of Washington, Seattle, Washington 98195, USA
[5]Department of Chemistry, University of California, Berkeley, California 94720, USA
[6]Department of Chemistry, Hiram College, Hiram, Ohio 44234, USA
[7]Centre for Atmospheric Chemistry and Chemistry Department, York University, Toronto, Ontario, M3J 1P3 Canada
[8]Department of Atmospheric and Oceanic Sciences, University of California, Los Angeles, California 90095, USA
[9]Department of Atmospheric Sciences, University of Washington, Seattle, Washington 98195, USA
[10]Department of Chemistry, University of Colorado, Boulder, Colorado 80309, USA
[*]now at: Department of Chemistry, University of York, York, YO10 5DD, UK
[**]now at: Department of Chemistry, Memorial University of Newfoundland, St. John's, Newfoundland, A1B 3X7, Canada

Correspondence to: S. S. Brown (steven.s.brown@noaa.gov)

Abstract.

High wintertime ozone levels have been observed in the Uintah Basin, Utah, a sparsely populated rural region with intensive oil and gas operations. The reactive nitrogen budget plays an important role in tropospheric ozone formation. Measurements were taken during three field campaigns in the winters of 2012, 2013, and 2014, which experienced varying climatic conditions. Average concentrations of ozone and total reactive nitrogen were observed to be 2.5 times higher in 2013 than 2012, with 2014 an intermediate year in most respects. However, photochemically active NO_x ($NO + NO_2$), remained remarkably similar all three years. Nitric acid comprised roughly half of NO_z ($\equiv NO_y - NO_x$) in 2013, with nighttime nitric acid formation through heterogeneous uptake of N_2O_5 contributing approximately 6 times more than daytime formation. In 2012, N_2O_5 and $ClNO_2$

were larger components of NO_z relative to HNO_3. The nighttime N_2O_5 lifetime between the high-ozone year 2013 and the low-ozone year 2012 is lower by a factor of 2.6, and much of this is due to higher aerosol surface area in the high ozone year of 2013. A box-model simulation supports the importance of nighttime chemistry on the reactive nitrogen budget, showing a large sensitivity of NO_x and ozone concentrations to nighttime processes.

1 Introduction

Wintertime ozone air pollution has recently been observed in several North American basins and currently represents one of the most severe air pollution problems in the United States (Schnell et al., 2009; Carter and Seinfeld, 2012; Helmig et al., 2014; Rappenglück et al., 2014; Oltmans et al., 2014; Edwards et al., 2014). It has been associated with emissions from oil and gas operations coupled with meteorological conditions that produce high surface albedo and temperature inversions, causing stable stagnation events. As with more conventional summertime urban air pollution, winter ozone production requires photochemistry of $NO_x (= NO + NO_2)$ and volatile organic compounds (VOCs). In polluted areas, such as the Uintah Basin, NO_x is emitted mainly from fossil fuel combustion and can further oxidize to form reactive nitrogen species such as HNO_3, acyl peroxynitrates (PAN), N_2O_5, NO_3, $ClNO_2$, organic nitrates, etc., which, together with NO_x, make up total reactive nitrogen (NO_y). Oxidation of NO_x occurs through different reaction pathways during the day than at night, but both contribute significantly to NO_y speciation. Some of these species tend to be permanent sinks of NO_x, such as HNO_3, whereas others such as PAN or N_2O_5 can act as temporary sinks (reservoirs) and revert to NO_x via photo- or thermochemistry. Thus, an understanding of the reactive nitrogen budget contributes to understanding ozone formation.

To study the conditions and precursors that cause these anomalous wintertime ozone events, we deployed a suite of ground based chemical, radiation and meteorological measurements as part of the Uintah Basin Winter Ozone Studies (UBWOS) in 2012, 2013 and 2014. The UBWOS studies in 2012 and 2013 experienced very different meteorological conditions and yielded strikingly different results. In 2012, the lack of snow cover and the associated shallow inversions produced ozone with average values that showed distinct photochemistry but did not approach the 75 ppbv 8 hour National Ambient Air Quality Standard (NAAQS), presenting a valuable baseline of chemical concentrations for this oil and gas-producing region (Edwards et al., 2013). In 2013, however, the snow cover resulted in strong temperature inversions, increased precursor concentrations, and increased photochemistry, which brought about elevated ozone levels (Edwards et al., 2014). The Horsepool measurement site in the Basin experienced exceedances of the ozone NAAQS on 20 out of the 28 days of measurement in 2013. In 2014 the conditions were intermediate both meteorologically and chemically. A direct comparison of 2012 with 2013 provides valuable insight into the key elements that cause high wintertime ozone. In this paper we focus on reactive nitrogen and its partitioning

during the two years to help explain the chemical processes that cause high ozone.

2 Field Campaigns and Measurement Techniques

The three successive campaigns were conducted on January 15 - February 27, 2012; January 23 - February 21, 2013; and January 28 - February 14, 2014 at the Horsepool site near Vernal, Utah. The site is located at 40.14370°N, 109.46718°W, 35 km south of Vernal, Utah, the largest city in the basin. The basin is mostly rural, with a total population of 50,000 concentrated mainly in three towns (Vernal, Roosevelt, and Duchesne). Approximately 10,000 producing oil/gas wells are spread throughout the basin, and the Horsepool measurement site is situated within the predominantly natural gas producing wells in the eastern half of the basin, as seen in Figure 1.

The suite of measurements over the three years varied but was very extensive every year, and descriptions can be found in the final reports for the Uintah Basin Ozone Studies on the website of the Utah Department of Environmental Quality (www.deq.utah.gov/locations/U/uintahbasin/ozone/overview.htm). A brief summary of the ambient gas-phase reactive nitrogen measurements is given here. During all three years, NO, $\mathrm{NO_2}$, $\mathrm{NO_3}$, and $\mathrm{N_2O_5}$ were measured using cavity ring-down spectroscopy (CRDS), which was also used in conjunction with thermal dissociation (TD-CRDS) to measure $\mathrm{NO_y}$ in 2013 and 2014 (Wild et al., 2014). In 2012, $\mathrm{NO_y}$ was measured using catalytic conversion to NO on a gold tube at 325 $^\circ\mathrm{C}$ with subsequent detection using chemiluminescence (CL) via the reaction with $\mathrm{O_3}$. Nitric and nitrous acids were measured with an acetate ion chemical ionization mass spectrometer (acid CIMS) all three years. Alkyl nitrates and peroxy nitrates were only measured in 2012, by thermally dissociating them to $\mathrm{NO_2}$ and subsequently detecting them via laser-induced fluorescence (TD-LIF). Acyl peroxynitrates (PANs) and nitryl chloride ($\mathrm{ClNO_2}$) were measured all three years using an iodide chemical ionization mass spectrometer ($\mathrm{I^-}$CIMS). Finally, there was extra focus on HONO in 2014, which was measured by a long-path differential optical absorption spectrometer (LP-DOAS), a broadband cavity-enhanced spectrometer (ACES), and a long-path absorption photometer (LoPAP), as well as the acid CIMS and the $\mathrm{I^-}$CIMS. The measurements and references for the techniques are summarized in Table 1. Due to the overlap or lack of some measurements in different years, not all the data were utilized in this analysis.

3 Results

3.1 Ozone and Reactive Nitrogen Levels

In this analysis we focus on analysis of diel profiles, averaged over the duration of each field campaign. This method highlights the general differences between the years but does not distinguish between different meteorological conditions within a campaign. In Figure 2, we show whole-campaign

diel averages of the ozone levels at the Horsepool ground site for the winters of 2012, 2013, and 2014. The dotted line shows the NAAQS level of 75 ppbv. On average, ozone levels were 2.5 times higher in 2013 than in 2012. Additionally, ozone production during midday (between the dotted lines at 09:45 and 14:30 hours) was 2.7 ppbv/hr in 2012 and 6.9 ppbv/hr in 2013, a factor of 2.6 higher. In 2014, the ozone levels were intermediate, with the daily increase at 4.8 ppbv/hr. Although the ozone increase is affected both by chemical production and dilution due to the changing boundary layer, chemical ozone production accounts for most of this increase at this site. For 2012, when atmospheric conditions were least stable, chemical production was estimated to account for 70-85% of the observed average diel rise in surface O_3. These estimates were derived from comparison of the model to the measured surface level rise and from measurements of the diel average O_3 profile at different heights up to 500 m from a tethered balloon. (Edwards et al., 2013).

The top plot in Figure 3 shows the diurnally averaged total reactive nitrogen (NO_y). The NO_y in 2013 is on average a factor of 2.5 higher than 2012, with 2014 again at intermediate levels. However, the middle plot of Figure 3 shows that the total NO_x concentrations are consistently similar for all three years, despite significantly different meteorological conditions and ozone production rates. The bottom plot shows the ratio NO_x/NO_y, a measure of the rate of oxidation of reactive nitrogen independent of dilution, whereby a lower ratio implies more oxidation. The large differences in this ratio (a factor 2.6 on average between 2012 and 2013) instead indicates large differences in levels of NO_x oxidation caused by changes in ambient chemistry, which caused the similarity of NO_x levels between the measurement years.

3.2 NO_y Partitioning and NO_x Oxidation

We examine the oxidation pathways and products in order to understand the different levels of NO_x oxidation for the various years. Figure 4 shows the partitioning of NO_z ($\equiv NO_y - NO_x$) for 2012 and 2013. In 2012, since NO_x makes up approximately 80% of NO_y, the subtraction to calculate NO_z results in a noisy trace with large uncertainty relative to the amount of NO_z present, and we instead take the sum of components to define total NO_z. This is not the case in 2013, and the "missing" part of NO_z is likely organic nitrates ($RONO_2$) for which we do not have a measurement.

Ammonium nitrate might be measured partially in the acid CIMS and the NO_y instrument due to heated inlets, and its contribution to NO_z has not been included in this analysis. Measurements of aerosol nitrate, which would include coarse mode aerosol whose source might not be excusively photochemical, present an average upper limit of 0.4 ppbv in 2012 and 1 ppbv in 2013. Nitrous acid, $HONO$, was measured as a small fraction (2.4%) of NO_z in 2012. Its mixing ratio was measured by both the acid CIMS and DOAS measurements, which both showed maximum values smaller than 120 pptv average at night and smaller during the day, with agreement to within a factor of 2. During 2013, the acid CIMS was the only measurement available. It showed very large signals at the mass normally interpreted as $HONO$ with a distinct, daytime maximum. As described in

Veres et al. (2015), HO_2NO_2 mixing ratios were observed to reach an average daytime maximum of approximately 4% of NO_z. Unpublished laboratory results suggest that a large fraction of the HO_2NO_2 is detected as HONO using the acid CIMS, resulting in a positive daytime bias in the 2013 measurements. Based on the similarity of DOAS HONO measurements in 2012 and 2014, HONO for 2013 was set equal to that from 2012. For further details on comparisons of HONO measurements, please see Edwards et al. (2014).

In 2012, N_2O_5 and $ClNO_2$ make up about half of the total NO_z budget at night, whereas they form a small percentage in 2013. Nitric acid (HNO_3) and PAN, however, make up about 75% of total NO_z throughout the whole diel cycle in 2013, with the inferred organic nitrates making up most of the remainder. The major oxidation pathways that produce these compounds during the day are:

$$NO_2 + OH + M \longrightarrow HNO_3 + M \quad \text{(R1)}$$

$$NO_2 + PA + M \longrightarrow PAN + M \quad \text{(R2)}$$

$$NO + RO_2 + M \xrightarrow{\alpha} RONO_2 + M \quad \text{(R3)}$$

where PA is the peroxyacetyl radical and includes all acyl peroxy radicals, with $CH_3C(O)O_2$ being the most important. The RO_2 include all other organic peroxy radicals, and α is the temperature-dependent yield of organic nitrates from the reaction of organic peroxy radical with NO, where the majority of this reaction produces an alkoxy radical and NO_2 (Lee et al., 2014). At night, when NO_3 is photochemically stable, the main pathway for NO_x oxidation is

$$NO_2 + O_3 \longrightarrow NO_3 + O_2 \quad \text{(R4)}$$

$$NO_3 + NO_2 + M \longrightarrow N_2O_5 + M \quad \text{(R5)}$$

This N_2O_5 can then further react heterogeneously to form nitric acid and nitryl chloride.

$$N_2O_5 + H_2O \xrightarrow{het} 2HNO_3 \quad \text{(R6)}$$

$$N_2O_5 + HCl \xrightarrow{het} HNO_3 + ClNO_2 \quad \text{(R7)}$$

Calculating the reaction rates of R1-5 allows us to compare NO_x loss rates (rates of conversion to NO_z) through these different pathways. The reaction rate constants are known, and the concentrations of OH and PA are supplied by a box model simulation using the master chemical mechanism (MCM), as is the production rate of organic nitrates. The MCM utilizes greater than 10^4 reactions, and the base run accurately reproduces an ozone buildup event in 2013 (Edwards et al., 2014). Additionally, the OH concentrations agree with OH inferred from VOC ratios (Koss et al., 2015) with average midday maximum OH levels calculated by the model to be approximately 1×10^6 cm^{-3}. During the 2012 study, calculated midday OH was 7×10^5 cm^{-3} (Edwards et al., 2013). Although PAN can thermally dissociate, the long lifetime at wintertime temperatures (>10 hours below $10^{\circ}C$) means we can effectively consider only the forward reaction. The limiting step in R4-5 is the $NO_2 + O_3$ reaction and we assume that the sequence of reactions in R4-7 quantitatively converts NO_2 to stable products, mainly HNO_3, at night in 2013 (we calculate N_2O_5 lifetimes to be <2

hours, see below). The NO_x loss rate due to R4 is doubled, because the sum of reactions R4 and R5 would lead to NO_x loss at twice the rate of R4. The reaction pathway to make N_2O_5 is negligible during daylight hours due to photodissociation of NO_3 together with the fast reaction of NO_3 with NO, and has been set to zero. The resulting 2013 NO_x loss rates due to reactions R1-5 are shown in Figure 5.

Separating the daytime and nighttime partitioning in Figure 4 highlights the species that are long-lived at night and short-lived during the day (N_2O_5 and $ClNO_2$), demonstrating the role of the nighttime species in reactive nitrogen chemistry. Nitric acid, PAN, and organic nitrates, on the other hand, are long-lived compared to a diel cycle, and we do not expect the nighttime or daytime average to reflect chemical production that is restricted to these periods. It instead represents an average not just over a diel cycle but over the whole campaign.

Integrating the diurnally averaged loss rates gives total daily calculated production of the three major components of NO_z, with the simplifying assumption that all N_2O_5 is converted to nitric acid (we estimate the $ClNO_2$ yield for 2012 and 2013 to be 11% and 2%, respectively). In Figure 6 we compare the partitioning of these integrated production rates with the measured partitioning of HNO_3, PAN, and inferred organic nitrates for 2013. Production rates and observed concentrations should not necessarily be proportional, depending on the loss mechanisms. For example, HNO_3 will be lost via dry deposition to the ground or snow surface such that its measured contribution to nitrogen partitioning may be smaller than that inferred from its production rate. However, the agreement between production rates and observations illustrates that our methods of treating the reactive nitrogen in the current analysis and in the MCM box model are self-consistent.

The reactions R1 and R4-7 result in formation of HNO_3, which makes up the bulk of NO_z in 2013. Furthermore, the integrated nighttime loss toward nitric acid is 5.9 times greater than during the day. Therefore much of the difference in NO_z between the low ozone year of 2012 and the high ozone year of 2013 must be due to a large difference in nighttime N_2O_5 reactivity, which we analyze below.

3.3 N_2O_5 Lifetimes

When the sinks of NO_3 are small compared to those of N_2O_5, and assuming an equilibrium state between NO_2, NO_3, and N_2O_5, the ratio of the N_2O_5 concentration to the production rate of NO_3 equals the N_2O_5 lifetime ($\tau_{N_2O_5}$),

$$\tau_{N_2O_5} = \frac{[N_2O_5]}{k \cdot [NO_2] \cdot [O_3]} \quad (1)$$

where k is the rate coefficient for reaction R4 (Brown et al., 2003). An analysis of the resulting lifetimes, which can be considered a measure of N_2O_5 reactivity, are shown with the solid lines in Figure 7. Since Equation 1 assumes a steady state in NO_3 and N_2O_5, the relevant period when this lifetime interpretation will be most valid is at the end of the night. However, a simple five reaction

chemical box model including NO_3 and N_2O_5 production and first-order loss (Brown et al., 2003) shows that it would take >20 hours to reach a steady state in 2012. After the 14 hours of night, we predict that the lifetime calculated using Equation 1 gives us 77% of the actual lifetime. In 2013, the model predicts that the system reaches 90% of steady state in 1.8 hours. The lifetimes in 2012 are a factor of approximately 2 times longer than in 2013, or 2.6 times if we use calculated equilibrium values. McLaren et al. (2010) have suggested an alternate method for lifetime analysis that explicitly takes the time derivative of N_2O_5 into account to correct its lifetime for failure to reach steady state. Figure 7 also shows the steady state lifetime calculated using this method using a smooth fit function for the N_2O_5 diel profile to calculate the derivative. Since the reaction of N_2O_5 occurs heterogeneously via uptake onto surfaces, the difference in lifetime between the two years could conceivably be due to higher aerosol surface area or faster ground deposition. The average value of the product of the $NO_3-N_2O_5$ equilibrium constant, $K_{eq}(T)$, and the NO_2 concentration ($K_{eq}[NO_2]$), equal to the predicted ratio of N_2O_5 to NO_3, was 115 and 440 during nighttime hours in 2012 and 2013, respectively. Late night average NO_3 of 2.2 pptv agreed well with the predicted equilibrium. Average predicted NO_3 of less than 0.5 pptv in 2013 could not be accurately measured. The late night average steady state lifetime of NO_3 in 2012 was approximately 100 s, while in 2013 it was 13 s. Under these cold conditions, the very short NO_3 lifetimes do not represent the reactivity of the NO_3-N_2O_5 system, which is dominated by heterogeneous loss of N_2O_5, and we provide them here for reference only.

Lifetimes due to aerosol can be calculated separately using measurements of aerosol surface area and the equation for heterogeneous uptake, assuming no limitation for gas phase diffusion (valid for small particle size and small to moderate uptake coefficients, and consistent with conditions from both 2012 and 2013):

$$\tau_{N_2O_5} = \left(\frac{1}{4}\gamma\,\bar{c}\,S_A\right)^{-1}, \quad (2)$$

where γ is the uptake coefficient, $\bar{c}$ the mean molecular speed, and S_A the surface area density of the aerosol. The aerosol surface area density was calculated from number size distributions measured using a Scanning Mobility Particle Sizer for particles between 20 and 500 nm geometric diameter, and an Aerodynamic Particle Sizer for particles between 0.7 and 10.37 μm. Size distribution measurements were taken at relative humidity $< 25\%$, and a hygroscopic growth factor was calculated using measurements of ambient humidity and aerosol composition (Bates et al., 2002). There are few determinations of N_2O_5 uptake coefficients in winter. During winter measurements in Colorado, Wagner et al. (2013) determined an average $\gamma = 0.02$ under similar conditions of temperature and relative humidity, and at a site with nearly identical latitude and elevation. Using $\gamma = 0.02$, we calculate the lifetimes of N_2O_5 due to aerosol uptake for 2012 and 2013, plotted as dashed lines in Figure 7. The 2012 lifetime includes a 10% correction from the contribution of losses due to VOCs (see below). On average, lifetimes calculated from aerosol uptake were a factor of 4.1 higher

in 2012 than 2013, compared to the factor 2.6 change in lifetime calculated from the N_2O_5 steady state of Equation 1 and the box model. However, an uptake factor of $\gamma = 0.026$ in 2012 would bring the lifetimes calculated using these two methods into agreement. Since we did not perform eddy covariance flux measurements, we do not know the deposition rate, and the γ values derived from comparison to the steady state lifetimes thus represent an upper limit. Additionally, since the lifetime of N_2O_5 is longer in 2012, the influence of deposition to the ground surface might be greater if it were roughly constant relative to other sinks that increased between 2012 and 2013. The change in aerosol uptake between the two years is in part due to the higher relative humidity measured in 2013, which increased the aerosol surface area through hygroscopic growth. The increased RH in 2013 caused frequent and persistent fog. Due to the difficulty in extrapolating a hygroscopic growth factor near saturation, data during periods of relative humidity above 95% have been excluded in this analysis. Hygroscopic growth associated with the higher relative humidity contributed a factor of approximately 1.3 to the difference in lifetime between the two years.

One condition of Equation 1 is that the major sink of NO_3 is through aerosol uptake via N_2O_5 instead of reactions with volatile organic compounds (VOCs). Previous studies in regionally polluted areas have shown that loss of NO_3 and N_2O_5 can be dominated by NO_3-VOC reactions, N_2O_5 uptake or a combination of the two (Aldener et al., 2006; Brown et al., 2011). Given the high VOC concentrations in the Uintah Basin (Helmig et al., 2014), we performed an analysis of NO_3 reactivity to quantify the contribution of NO_3 chemistry to the lifetime of N_2O_5. The loss due to VOC is simply the sum of all the NO_3-VOC rate constants (k_i) times the measured VOC concentrations

$$k_{loss}\left(NO_3\right) = \sum_i k_i \left[VOC_i\right] \tag{3}$$

This first order loss rate coefficient for NO_3 can be compared to the first order loss rate coefficient for uptake of N_2O_5 to aerosol by dividing the former by the equilibrium ratio of N_2O_5/NO_3 (Brown et al., 2003). VOC measurements by proton transfer reaction mass spectrometry and gas chromatography in 2012 provided measurements of a more extensive VOC suite than the measurements in 2013, so VOC ratios from 2012 were used to estimate some compounds missing from 2013 measurements, as was done by Edwards et al. (2013). The calculations show that with an N_2O_5 uptake coefficient of 0.02, NO_3 losses due to reactions with VOCs were approximately 10 times less than N_2O_5 uptake to aerosol in 2012, and approximately 40 times less in 2013. A lower N_2O_5 uptake coefficient would increase the fraction of the NO_3 and N_2O_5 reactivity attributable to NO_3-VOC chemistry. However, the comparisons of Figure 7 suggest that the average N_2O_5 uptake coefficient is not appreciably smaller than 0.02. Figure 8 shows the relative loss rates, as well as the breakdown of reactivity with different classes of VOCs. During both years, reactivity with alkanes form the major part of NO_3 loss to VOCs (45-51%). To our knowledge, this is the first instance in which alkanes have been determined as the largest single component of NO_3-VOC reactivity in ambient air. For example, studies in other locations, such as Houston, Texas, show that alkanes contribute

approximately 1% to ambient NO_3 reactivity (Brown et al., 2011). Despite their very slow rate constants for reaction with NO_3, alkanes make up an overwhelming fraction of the measured VOC composition in the Uintah Basin, leading to an unusually large contribution to NO_3 reactivity. Isoprene and dimethyl sulfide (DMS) are collectively labeled "biogenic" according to convention, but due to winter conditions we anticipate no biogenic source for these compounds. Rather, we assume both to be emissions from oil and gas operations. For example, an anthropogenic source of isoprene may be emitted in small quantities in vehicle exhaust (McLaren et al., 1996), while DMS may be a component of the reduced sulfur emissions from natural gas. In any case, the measured concentrations of both compounds are small (2 pptv and 0.7 pptv, respectively, nighttime average in 2013), and their contribution to NO_3 reactivity represents the fast NO_3 rate constant with these species. It is possible that other highly reactive but unmeasured VOCs contribute to the NO_3 reactivity. For example, Crowley et al. (2011) report an important role for reduced sulfur species other than DMS in loss of NO_3 radicals near an oil refinery. Such measurements were unavailable for the UBWOS studies.

Since N_2O_5 uptake to the ground can also affect lifetimes, one has to consider differences in inlet height and ground composition between different years. In 2012, N_2O_5 was measured from a scaffold tower at a height of 11 meters, whereas in 2013, the lack of such a tower limited us to a sampling height of 4 meters. To investigate a possible N_2O_5 gradient, we alternately sampled from 14 m and 1 m during the final weeks of the 2014 campaign, spanning the sample heights of the 2012 and 2013 inlets. In 2014, the ground was snow-covered, and conditions generally resembled 2013 more than 2012. The resulting lifetime calculations using NO_3 production rates (Equation 1) are shown in Figure 9 with black solid and dotted lines. We measured roughly twice the N_2O_5 lifetime at the high inlet as compared to the low inlet. This difference results solely from differences in N_2O_5 concentrations; measurements of NO_2, O_3 and aerosol surface area between 4 and 14 meters did not show significant differences at night and were assumed to be equal for the lifetime calculation. Ground deposition of N_2O_5 can form an important contribution to the lifetime (Huff et al., 2011; Kim et al., 2014), but the year-to-year variability is a significantly larger effect than the measured N_2O_5 gradient. This suggests that nighttime aerosol uptake of N_2O_5 could play a major role in NO_x oxidation and contributes to keeping NO_x levels similar between the three years.

4 Sensitivity of NO_x and O_3 to NO_x oxidation pathways

We again used the MCM box model simulation to investigate the relative sensitivities of nitrogen oxide loss and O_3 production rates to some of the different NO_x oxidation pathways discussed above. We increased/decreased the reaction rate constants of reactions R1 ($NO_2 + OH$), R2 ($NO_2 + PA$), and R4 ($NO_2 + O_3$) by a factor of 2, keeping all else equal, and compared the resulting NO_x and ozone levels after the model stabilized to the base simulation results that matched observations. The

base simulation included a continuous source of NO_x, tuned to match observed levels (Edwards et al., 2014). In the MCM, the rate of reaction R6 was set empirically to match the observed N_2O_5 concentrations. The resulting rate was fast enough that reaction R4 was the rate-limiting step in the reaction pathway R4-R7, and was therefore used to test the sensitivity of that pathway.

The results are shown in Figure 10, with the left panel showing the final day of the simulation, and the right panel comparing the final day's 24-hour averages. For reactions R1 and R2, an increased/decreased rate has very little effect on NO_x once the model has stabilized. The nighttime pathway has a much larger effect, however, and an doubled rate leads to a 28% NO_x reduction. Halving the rate causes a 43% increase. During the day, changing the rate of R4 has no effect due to the fast photodissociation of NO_3. The response of O_3 concentrations is also shown, with the nighttime reactions having the greatest effect. Changing PAN and HNO_3 production have comparable effects on ozone even though the effective NO_x removal rates are approximately 4 times different. This may be because the $OH + NO_2$ affects the propagation of the HO_x cycle directly with OH either reacting with NO_2 or a VOC. PAN production, on the other hand, has its effect based on whether PA reacts with NO or NO_2, which scales as the ratio of PA loss to NO vs loss to NO_2.

Although organic nitrates are the largest photochemical pathway for nitrogen loss, we did not perform an analogous simulation using reaction R3 ($NO + RO_2$). Since a comparable simulation involves changing all the rate coefficients for a large number of reactions, performing these simulations are beyond the scope of this paper. However, if we scale the sensitivity of doubling/halving the reaction rates for organic nitrate production to the sensitivity to daytime production of nitric acid (a factor of 4.6), we get a change in NO_x of approximately 7% and a change in O_3 of approximately 17%. The effect could be larger since NO_x is higher in the morning when the $RO_2 + NO$ rate is largest. Scaling it to PAN production (R2) causes a change in NO_x and O_3 of approximately 3% and 6%, respectively. If instead we were to scale α by a factor of two, the effect could be larger since there is no competition for the fate of RO_2; every RO_2 reacts with NO. For example, Lee et al. (2014) found that a 50% increase in α results in a 7 ppb decrease in ozone (at an ozone concentration of $\sim$60 ppbv), and they estimate a 25 ppbv effect (at $\sim$140 ppbv ozone) for conditions with higher J values and slower mixing. Thus, although organic nitrate production should have the largest influence of the photochemical NO_x loss mechanisms on both NO_x and O_3, we anticipate that it still has a smaller effect on NO_x loss pathways than the nighttime chemistry in this winter environment.

Winter O_3 should be more sensitive to N_2O_5 chemistry because it is predominant during winter conditions, with low primary radical generation during daytime and longer duration of darkness. The majority of polluted winter conditions do not produce O_3 efficiently due to low photochemical radical production rates. These systems are typically NO_x saturated (Edwards et al., 2013, 2014; Kleinman, 2005). The result of N_2O_5 chemistry in most of these situations would be to increase O_3 photochemistry during the daytime by reducing the NO_x levels overnight. In summertime ur-

ban environments, N_2O_5 chemistry should have an effect, but it would be smaller because it will consume a smaller fraction of reactive nitrogen compared especially to reaction R1 in more typical summertime ozone photochemical systems. Its effect on O_3 will be highly sensitive to the O_3-NO_x sensitivity in any given region, and would be difficult to generalize.

The influence of $ClNO_2$ production from N_2O_5 is not explicitly considered here, and was determined to be a small effect on NO_x due to its low yield. However, it may be an important effect on O_3 production in other regions during both summer and winter, especially if $ClNO_2$ photolysis is a larger contribution to photochemical radicals than was determined for the UBWOS 2013 study.

5 Conclusions

The measurements at Horsepool in the Uintah Basin, Utah, during the winters of 2012, 2013, and 2014 and subsequent modeling provide much insight into the fate of reactive nitrogen and its relationship to ozone production in the basin. Ozone levels were highly elevated in 2013 compared to 2012, with 2.5 times more ozone on average and 20 out of the 28 days of the measurements at Horsepool experiencing exceedances of the 75 ppbv 8-hour-average daily maximum NAAQS. Total reactive nitrogen, NO_y, was 2.5 times more concentrated in 2013, yet photochemically active NO_x concentrations were approximately equal all three years. This resulted from very different rates of NO_x oxidation leading to much higher concentrations of HNO_3, PAN, and missing NO_y, presumed to be organic nitrates, with HNO_3 making up the largest part of the NO_z budget. Much of the HNO_3 formed during the night, with integrated NO_2 loss toward HNO_3 approximately 6 times higher at night than during the day. At night, HNO_3 is produced via heterogeneous uptake of N_2O_5 onto aerosol, and calculations using measurements of aerosol surface area reproduce the differences in lifetime as calculated using NO_3 production rates. Some of the N_2O_5 is lost to ground deposition, but aerosol uptake forms a major component of HNO_3 formation. A box model simulation confirms that the nighttime N_2O_5 heterogeneous reactions play a significant role in NO_x chemistry and related ozone production.

Acknowledgements. The Uintah Basin Winter Ozone Studies were a joint project led and coordinated by the Utah Department of Environmental Quality (UDEQ) and supported by the Uintah Impact Mitigation Special Service District (UIMSSD), the Bureau of Land Management (BLM), the Environmental Protection Agency (EPA) and Utah State University. This work was funded in part by the Western Energy Alliance, and NOAA's Atmospheric Chemistry, Climate and Carbon Cycle program. We thank Questar Energy Products for site preparation and support. This is PMEL contribution number 4353.

References

Aldener, M., Brown, S. S., Stark, H., Williams, E. J., Lerner, B. M., Kuster, W. C., Goldan, P. D., Quinn, P. K., Bates, T. S., Fehsenfeld, F. C., and Ravishankara, A. R.: Reactivity and loss mechanisms of NO_3 and N_2O_5 in a polluted marine environment: Results from in situ measurements during New England Air Quality Study 2002, Journal of Geophysical Research: Atmospheres, 111, D23S73, 2006.

Bates, T. S., Coffman, D. J., Covert, D. S., and Quinn, P. K.: Regional marine boundary layer aerosol size distributions in the Indian, Atlantic, and Pacific Oceans: A comparison of INDOEX measurements with ACE-1, ACE-2, and Aerosols99, Journal of Geophysical Research: Atmospheres, 107, INX2 25–1–INX2 25–15, 2002.

Brown, S. S., Stark, H., and Ravishankara, A. R.: Applicability of the steady state approximation to the interpretation of atmospheric observations of NO_3 and N_2O_5, Journal of Geophysical Research: Atmospheres, 108, 4539, 2003.

Brown, S. S., Dubé, W. P., Peischl, J., Ryerson, T. B., Atlas, E., Warneke, C., de Gouw, J. A., te Lintel Hekkert, S., Brock, C. A., Flocke, F., Trainer, M., Parrish, D. D., Feshenfeld, F. C., and Ravishankara, A. R.: Budgets for nocturnal VOC oxidation by nitrate radicals aloft during the 2006 Texas Air Quality Study, Journal of Geophysical Research: Atmospheres, 116, D24305, 2011.

Carter, W. P. and Seinfeld, J. H.: Winter ozone formation and VOC incremental reactivities in the Upper Green River Basin of Wyoming, Atmospheric Environment, 50, 255 – 266, 2012.

Crowley, J. N., Thieser, J., Tang, M. J., Schuster, G., Bozem, H., Beygi, Z. H., Fischer, H., Diesch, J.-M., Drewnick, F., Borrmann, S., Song, W., Yassaa, N., Williams, J., Pöhler, D., Platt, U., and Lelieveld, J.: Variable lifetimes and loss mechanisms for NO_3 and N_2O_5 during the DOMINO campaign: contrasts between marine, urban and continental air, Atmospheric Chemistry and Physics, 11, 10 853–10 870, 2011.

Day, D. A., Wooldridge, P. J., Dillon, M. B., Thornton, J. A., and Cohen, R. C.: A thermal dissociation laser-induced fluorescence instrument for in situ detection of NO_2, peroxy nitrates, alkyl nitrates, and HNO_3, Journal of Geophysical Research: Atmospheres, 107, ACH 4–1–ACH 4–14, 2002.

Edwards, P. M., Young, C. J., Aikin, K., deGouw, J., Dubé, W. P., Geiger, F., Gilman, J., Helmig, D., Holloway, J. S., Kercher, J., Lerner, B., Martin, R., McLaren, R., Parrish, D. D., Peischl, J., Roberts, J. M., Ryerson, T. B., Thornton, J., Warneke, C., Williams, E. J., and Brown, S. S.: Ozone photochemistry in an oil and natural gas extraction region during winter: simulations of a snow-free season in the Uintah Basin, Utah, Atmospheric Chemistry and Physics, 13, 8955–8971, 2013.

Edwards, P. M., Brown, S. S., Roberts, J. M., Ahmadov, R., Banta, R. M., deGouw, J. A., Dubé, W. P., Field, R. A., Flynn, J. H., Gilman, J. B., Graus, M., Helmig, D., Koss, A., Langford, A. O., Lefer, B. L., Lerner, B. M., Li, R., Li, S.-M., McKeen, S. A., Murphy, S. M., Parrish, D. D., Senff, C. J., Soltis, J., Stutz, J., Sweeney, C., Thompson, C. R., Trainer, M. K., Tsai, C., Veres, P. R., Washenfelder, R. A., Warneke, C., Wild, R. J., Young, C. J., Yuan, B., and Zamora, R.: High winter ozone pollution from carbonyl photolysis in an oil and gas basin, Nature, 514, 351–354, 2014.

Heland, J., Kleffmann, J., Kurtenbach, R., and Wiesen, P.: A new instrument to measure gaseous nitrous acid (HONO) in the atmosphere, Environmental Science & Technology, 35, 3207–3212, 2001.

Helmig, D., Thompson, C. R., Evans, J., Boylan, P., Hueber, J., and Park, J.-H.: Highly Elevated Atmospheric Levels of Volatile Organic Compounds in the Uintah Basin, Utah, Environmental Science & Technology, 48,

4707–4715, http://pubs.acs.org/doi/abs/10.1021/es405046r, 2014.

Huff, D., Joyce, P., Fochesatto, G., and Simpson, W.: Deposition of dinitrogen pentoxide, N_2O_5, to the snowpack at high latitudes, Atmospheric Chemistry and Physics, 11, 4929–4938, 2011.

Kim, M. J., Farmer, D. K., and Bertram, T. H.: A controlling role for the air- sea interface in the chemical processing of reactive nitrogen in the coastal marine boundary layer, Proceedings of the National Academy of Sciences, 111, 3943–3948, 2014.

Kleinman, L. I.: The dependence of tropospheric ozone production rate on ozone precursors, Atmospheric Environment, 39, 575–586, 2005.

Koss, A. R., de Gouw, J., Warneke, C., Gilman, J. B., Lerner, B. M., Graus, M., Yuan, B., Edwards, P., Brown, S. S., Wild, R., Roberts, J. M., Bates, T. S., and Quinn, P. K.: Photochemical aging of volatile organic compounds associated with oil and natural gas extraction in the Uintah Basin, UT, during a wintertime ozone formation event, Atmospheric Chemistry and Physics, 15, 5727–5741, 2015.

Lee, L., Wooldridge, P. J., Gilman, J. B., Warneke, C., de Gouw, J., and Cohen, R. C.: Low temperatures enhance organic nitrate formation: evidence from observations in the 2012 Uintah Basin Winter Ozone Study, Atmospheric Chemistry and Physics, 14, 12 441–12 454, 2014.

McLaren, R., Singleton, D. L., Lai, J. Y. K., Khouw, B., Singer, E., Wu, Z., and Niki, H.: Analysis of motor vehicle sources and their contribution to ambient hydrocarbon distributions at urban sites in Toronto during the Southern Ontario Oxidants Study, Atmospheric Environment, 30, 2219–2232, 1996.

McLaren, R., Wojtal, P., Majonis, D., McCourt, J., Halla, J. D., and Brook, J.: NO_3 radical measurements in a polluted marine environment: links to ozone formation, Atmospheric Chemistry and Physics, 10, 4187–4206, 2010.

Oltmans, S., Schnell, R., Johnson, B., Pétron, G., Mefford, T., and Neely, III, R.: Anatomy of wintertime ozone associated with oil and natural gas extraction activity in Wyoming and Utah, Elem. Sci. Anth., 2, 000 024, 2014.

Osthoff, H. D., Roberts, J. M., Ravishankara, A. R., Williams, E. J., Lerner, B. M., Sommariva, R., Bates, T. S., Coffman, D., Quinn, P. K., Dibb, J. E., Stark, H., Burkholder, J. B., Talukdar, R. K., Meagher, J., Fehsenfeld, F. C., and Brown, S. S.: High levels of nitryl chloride in the polluted subtropical marine boundary layer, Nature Geoscience, 1, 324–328, 2008.

Platt, U. and Stutz, J.: Differential Optical Absorption Spectroscopy, Principles and Applications, 2008.

Rappenglück, B., Ackermann, L., Alvarez, S., Golovko, J., Buhr, M., Field, R. A., Soltis, J., Montague, D. C., Hauze, B., Adamson, S., Risch, D., Wilkerson, G., Bush, D., Stoeckenius, T., and Keslar, C.: Strong wintertime ozone events in the Upper Green River basin, Wyoming, Atmospheric Chemistry and Physics, 14, 4909–4934, 2014.

Roberts, J. M., Veres, P., Warneke, C., Neuman, J. A., Washenfelder, R. A., Brown, S. S., Baasandorj, M., Burkholder, J. B., Burling, I. R., Johnson, T. J., Yokelson, R. J., and de Gouw, J.: Measurement of HONO, HNCO, and other inorganic acids by negative-ion proton-transfer chemical-ionization mass spectrometry (NI-PT-CIMS): application to biomass burning emissions, Atmospheric Measurement Techniques, 3, 981–990, 2010.

Schnell, R. C., Oltmans, S. J., Neely, R. R., Endres, M. S., Molenar, J. V., and White, A. B.: Rapid photochemical production of ozone at high concentrations in a rural site during winter, Nature Geoscience, 2, 120–122,

2009.

Slusher, D. L., Huey, L. G., Tanner, D. J., Flocke, F. M., and Roberts, J. M.: A thermal dissociation–chemical ionization mass spectrometry (TD-CIMS) technique for the simultaneous measurement of peroxyacyl nitrates and dinitrogen pentoxide, Journal of Geophysical Research: Atmospheres, 109, D19315, 2004.

Veres, P. R., Roberts, J. M., Wild, R. J., Edwards, P. M., Brown, S. S., Bates, T. S., Quinn, P. K., Johnson, J. E., Zamora, R. J., and de Gouw, J.: Peroxynitric acid (HO_2NO_2) measurements during the UBWOS 2013 and 2014 studies using iodide ion chemical ionization mass spectrometry, Atmospheric Chemistry and Physics, 15, 8101–8114, 2015.

Wagner, N. L., Dubé, W. P., Washenfelder, R. A., Young, C. J., Pollack, I. B., Ryerson, T. B., and Brown, S. S.: Diode laser-based cavity ring-down instrument for NO_3, N_2O_5, NO, NO_2 and O_3 from aircraft, Atmospheric Measurement Techniques, 4, 1227–1240, 2011.

Wagner, N. L., Riedel, T. P., Young, C. J., Bahreini, R., Brock, C. A., Dubé, W. P., Kim, S., Middlebrook, A. M., Öztürk, F., Roberts, J. M., Russo, R., Sive, B., Swarthout, R., Thornton, J. A., VandenBoer, T. C., Zhou, Y., and Brown, S. S.: N_2O_5 uptake coefficients and nocturnal NO_2 removal rates determined from ambient wintertime measurements, Journal of Geophysical Research: Atmospheres, 118, 9331–9350, 2013.

Wild, R. J., Edwards, P. M., Dubé, W. P., Baumann, K., Edgerton, E. S., Quinn, P. K., Roberts, J. M., Rollins, A. W., Veres, P. R., Warneke, C., Williams, E. J., Yuan, B., and Brown, S. S.: A Measurement of Total Reactive Nitrogen, NO_y, together with NO_2, NO, and O_3 via Cavity Ring-down Spectroscopy, Environmental Science & Technology, 48, 9609–9615, 2014.

Williams, E. J., Baumann, K., Roberts, J. M., Bertman, S. B., Norton, R. B., Fehsenfeld, F. C., Springston, S. R., Nunnermacker, L. J., Newman, L., Olszyna, K., Meagher, J., Hartsell, B., Edgerton, E., Pearson, J. R., and Rodgers, M. O.: Intercomparison of ground-based NO_y measurement techniques, Journal of Geophysical Research: Atmospheres, 103, 22 261–22 280, 1998.

Young, C. J., Washenfelder, R. A., Roberts, J. M., Mielke, L. H., Osthoff, H. D., Tsai, C., Pikelnaya, O., Stutz, J., Veres, P. R., Cochran, A. K., VandenBoer, T. C., Flynn, J., Grossberg, N., Haman, C. L., Lefer, B., Stark, H., Graus, M., de Gouw, J., Gilman, J. B., Kuster, W. C., and Brown, S. S.: Vertically resolved measurements of nighttime radical reservoirs in Los Angeles and their contribution to the urban radical budget, Environmental Science & Technology, 46, 10 965–10 973, 2012.

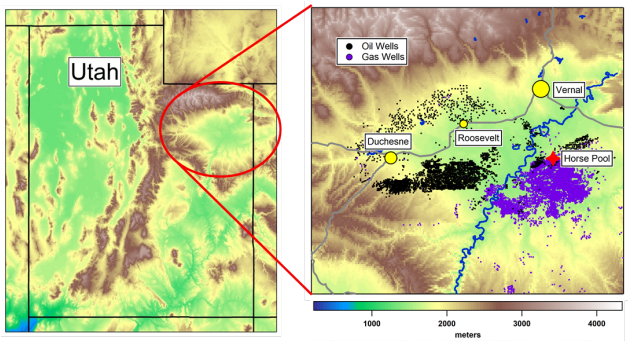

Fig. 1. Map of the Uintah Basin in Utah, showing the Horsepool measurement site, active oil and gas wells, and the major population centers. The background is colored by elevation as shown by the color bar.

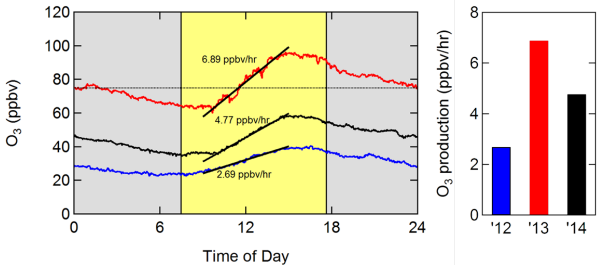

Fig. 2. Diel averages of ozone mixing ratios during the campaigns in 2012 (45 days), 2013 (28 days), and 2014 (27 days), and the 75 ppbv NAAQS for reference. Average ozone levels were 2.5 times higher in 2013 than 2012. Linear fits to the midday ozone increase illustrates the difference in average daily ozone production, plotted on the right.

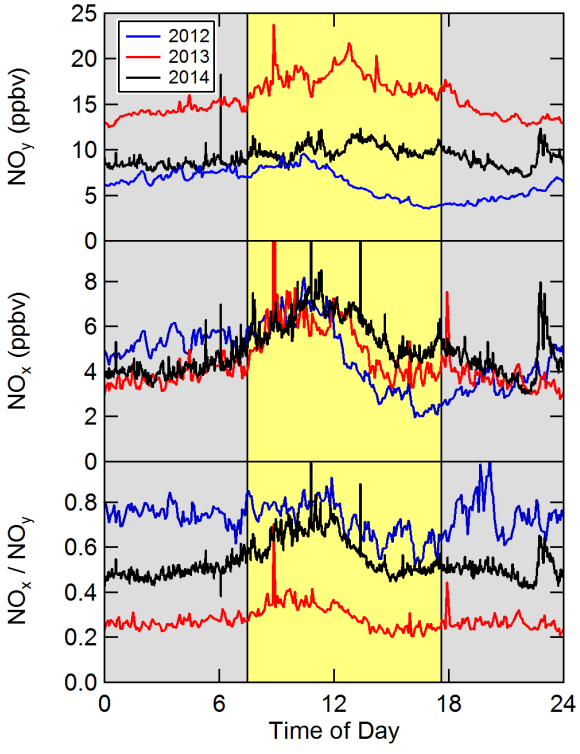

Fig. 3. Diel averages of reactive nitrogen. Top: Total NO_y was a factor of 2.5 times larger in 2013 than in 2012. Middle: The amount of photochemically active NO_x remained at similar levels all three years. Bottom: The ratio of NO_x/NO_y, an inverse measure of the level of oxidation of reactive nitrogen, was a factor of 2.6 smaller in 2013 than 2012.

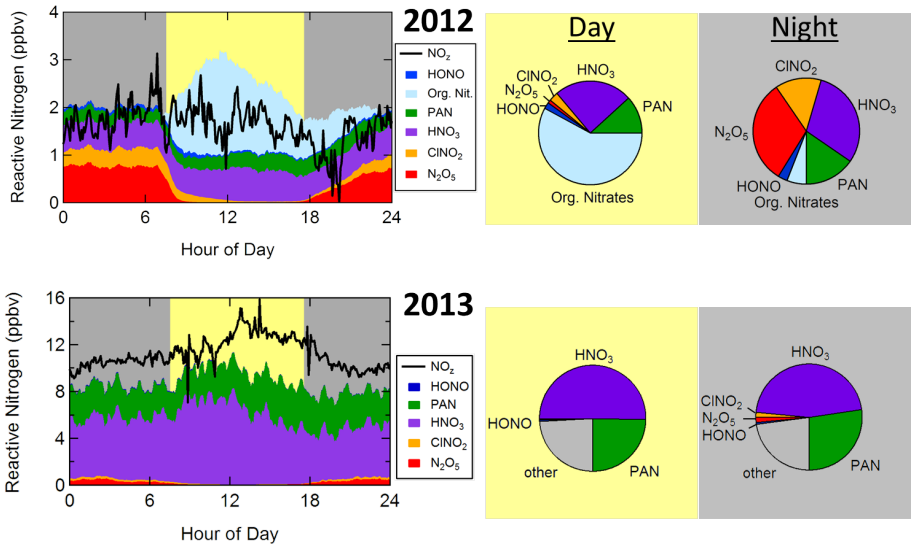

Fig. 4. Partitioning among reactive nitrogen species for 2012 and 2013, shown as diel averages (left) as well as daytime and nighttime pie charts (right). We take total NO_z to be the sum of components in 2012, and the difference between NO_y and NO_x in 2013. The missing NO_z in 2013 (labeled "other" in the pie charts) is likely organic nitrates, for which we do not have measurements in 2013. In 2012, daytime organic nitrates and nighttime N_2O_5 and $ClNO_2$ play an important role compared to 2013, where total PANs and HNO_3 are the largest contributors to NO_z.

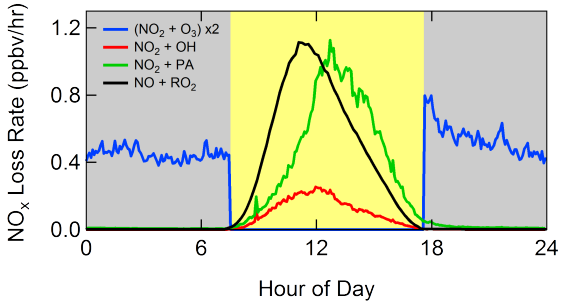

Fig. 5. Daytime and nighttime loss rates of NO_x in 2013 through the major oxidation pathways. Concentrations of OH, PA, and the production rate of organic nitrates ($NO + RO_2$) were supplied by the Master Chemical Mechanism box model used by Edwards et al. (2013). The daytime NO_3 production is set to zero because of the fast NO_3 photolysis and reaction with photochemically generated NO, and doubled at night due to reaction R5. The integrated nighttime loss toward HNO_3 is 5.9 times greater than during the day.

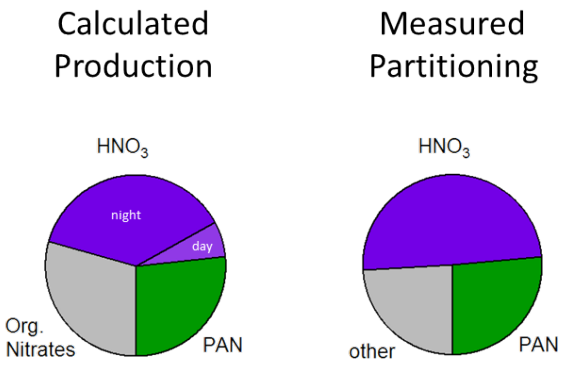

Fig. 6. Comparison of the relative importance in 2013 of calculated oxidized reactive nitrogen production rates to the measured NO_z partitioning for the three largest components of NO_z. On the right chart, "other" refers to the missing NO_z which we attribute to the unmeasured organic nitrates.

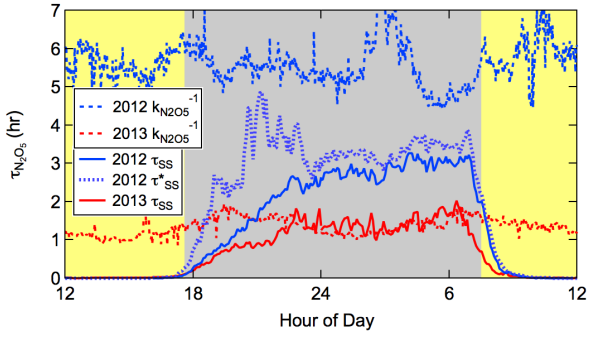

Fig. 7. Lifetimes of N_2O_5, calculated using the production rate of NO_3 (solid lines), the lifetime calculated using the method of McLaren et al. (2010) for 2012 (short dashed line, see text), and uptake to aerosol using an uptake coefficient of $\gamma = 0.02$ (dashed lines). In 2012 we expect that the calculation gives 77% of the actual lifetime, due to the system not reaching equilibrium at the end of the night. The McLaren method, based on explicit inclusion of the time derivative for N_2O_5, partially corrects for this effect, especially early in the night. An uptake coefficient of $\gamma = 0.026$ would bring the P(NO_3) and aerosol calculations in 2012 into agreement. The observed lifetimes from P(NO_3) include deposition, but the calculated curves do not.

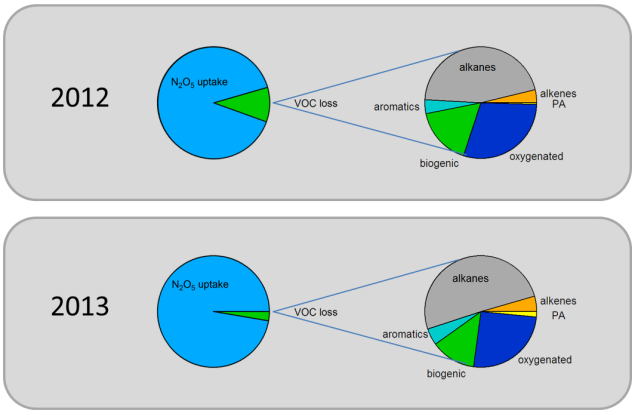

Fig. 8. Contributions to NO_3 reactivity. In both years, formation of N_2O_5 and consequent uptake to aerosol dominate NO_3 loss, and reactions with VOCs are primarily with alkanes. For comparison, the total NO_3 loss rate was 0.016 s^{-1} in 2012 and 0.118 s^{-1} in 2013.

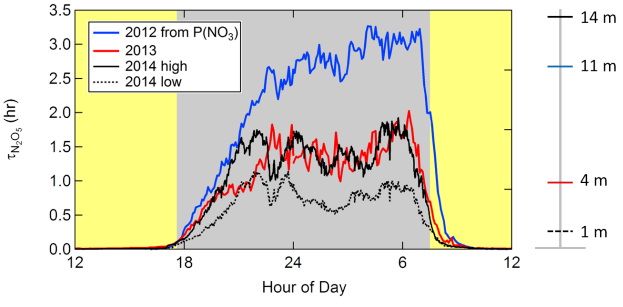

Fig. 9. The effect of inlet height on calculated lifetimes. Red and blue lines are the same as in Figure 7. Black lines are calculated from 2014 measurements with the solid line from an inlet at 14 meters and the dashed line from an inlet at 1 meter. These inlet heights span the inlets in 2012 at 11 meters and 2013 at 4 meters.

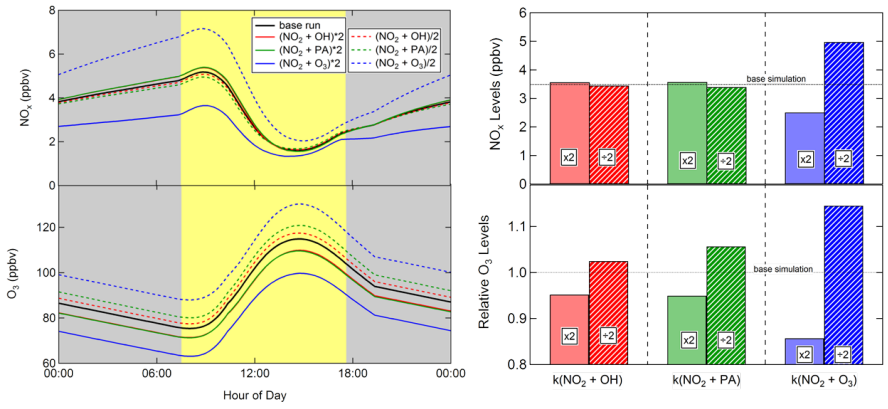

Fig. 10. The effect on NO_x and ozone concentration of changing the rates of select reactions in a box model simulation. The reaction $NO_2 + O_3$ represents the nighttime reaction pathway to HNO_3.

Table 1. Measurements of ambient gas-phase reactive nitrogen levels during UBWOS 2012-2014. The method abbreviations are described in Section 2, and LOD refers to the Limit of Detection. Not all measurements were used in this analysis.

Species Measured	Campaign Year			Method	Accuracy	LOD	Reference
	'12	'13	'14		%	pptv	
NO, NO_2, NO_3, N_2O_5	x	x	x	CRDS	5-10	1-100	Wagner et al. (2011)
NO_y	x			CL	20	10-100	Williams et al. (1998)
NO_y		x	x	TD-CRDS	10	20	Wild et al. (2014)
$HNO_3, HONO$	x	x	x	acid CIMS	30	10	Roberts et al. (2010)
alkyl & peroxy nitrates	x			TD-LIF	20	24-34	Day et al. (2002)
acyl peroxynitrates	x	x	x	I^-CIMS	20	10	Slusher et al. (2004)
$ClNO_2$	x	x	x	I^-CIMS	20	5	Osthoff et al. (2008)
HO_2NO_2			x	I^-CIMS	20	5	Veres et al. (2015)
$NO_2, NO_3, HONO$	x		x	LP-DOAS	3-8	80, 2, 20	Platt and Stutz (2008)
$NO_2, HONO$			x	ACES	15	200	Young et al. (2012)
$HONO$			x	LoPAP	15	10	Heland et al. (2001)